International Journal of Mass Spectrometry 304 (2011) 91–97

International Journal of Mass Spectrometry

journal homepage: www.elsevier.com/locate/ijms

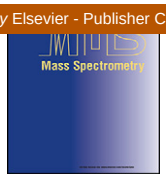

Identification, localization, and relative quantitation of pseudouridine in RNA by tandem mass spectrometry of hydrolysis products

Monika Taucher, Barbara Ganisl, Kathrin Breuker*

Institute of Organic Chemistry and Center for Molecular Biosciences (CMBI), University of Innsbruck, Innrain 52a, A-6020 Innsbruck, Austria

ARTICLE INFO

Article history:
Available online 4 June 2010

Keywords:
RNA
Pseudouridine
CAD
EDD

ABSTRACT

The constitutional isomers uridine (U) and pseudouridine (Ψ) cannot be distinguished from each other by simple mass measurements of RNA or its fragments because the conversion of U into Ψ is a "mass-silent" post-transcriptional modification. Here we propose a new mass spectrometry based method for identification, localization, and relative quantitation of Ψ in RNA consisting of ~20 nucleotides that does not require chemical labeling. Our approach takes advantage of the different fragmentation behavior of uridine (N-glycosidic bond) and pseudouridine (C-glycosidic bond) residues in RNA upon collisionally activated dissociation.

1. Introduction

The conversion by enzymes of uridine (U) into pseudouridine (Ψ) is one of the most common post-transcriptional modifications of ribonucleic acids (RNA) [1–4]. Clustering of Ψ residues in functionally relevant regions and a high degree of conservation throughout phylogeny indicate an important role of this modification in cellular processes, nevertheless, the biochemical function of pseudouridylation is not yet understood [3]. A prerequisite for making out the meaning of pseudouridylation is to identify where, when, and to what extent the modification occurs. As reviewed by Durairaj and Limbach [4], current biochemical methods for mapping pseudouridines in RNA are based on the technique introduced by Bakin and Ofengand [5] in 1993, utilizing chemical labeling reactions and reverse-transcriptase assays. In this widely used approach, transcription of RNA into DNA is terminated at such chemically labeled pseudouridines, which can be visualized in a gel of the DNA transcripts. Serious limitations of this method include the termination of transcription at other modified residues, and the requirement of RNA primer binding sites for the reverse-transcriptase enzyme [4]. Mass spectrometry (MS) is a powerful method for the detection and localization of post-transcriptional modifications in RNA [6–10], and the idea presents itself to use MS methodology instead of reverse-transcriptase assays for identification and localization of pseudouridines.

The conversion of U into Ψ is "mass-silent", meaning that pseudouridylation changes neither the mass of the RNA nor that of the modified residue (Scheme 1). Consequently, the majority of mass spectrometry based methods for identification and localization of pseudouridine in RNA relies on covalent attachment of chemical labels using reagents such as N-cyclohexyl-N′-β-(4-methylmorpholinium)ethylcarbodiimide p-tosylate (CMCT) or acrylonitrile [4,11–13]. However, protocols for chemical labeling of pseudouridine are generally laborious, and can suffer from limited selectivity [6].

A mass spectrometry based method for detection and sequence placement of Ψ in small RNA (≤15 nucleotides, nt) that does not involve chemical labeling has been developed in the McCloskey group [2]. Detection of Ψ was accomplished by multiple reaction monitoring (MRM) of small fragment ions (<250 Da) characteristic for pseudouridine [2]. Sequence placement of Ψ was inferred from enhanced abundance of *a*- and *w*- or *y*-type ions, and from the absence of (*a*-base) ions, from backbone cleavage next to the site of pseudouridylation in collisionally activated dissociation (CAD) experiments [2]. The above methodology indirectly monitors the presence of pseudouridines by taking advantage of the fact that the C-glycosidic bond of Ψ residues may effect somewhat different backbone fragment ion patterns than the N-glycosidic bond of U residues.

Tromp and Schürch studied CAD of 12 and 14 nt RNA, in which one and three of the nucleobases were replaced by biphenyl groups with C-glycosidic bonds, respectively [14]. The preferred fragmentation channel of the $(M-3H)^{3-}$ ions of 12 nt RNA (0.25 charges/nt) and $(M-4H)^{4-}$ ions of 14 nt RNA (0.29 charges/nt) was dissociation into *c* and *y* ions, and "no difference in gas-phase dissociation was found between unmodified nucleotides and biphenyl-modified building blocks" [14]. Apparently, the major backbone fragmentation channel of multiply deprotonated RNA into *c* and *y* ions is not affected by the nucleobases or the nature of the glycosidic bond.

* Corresponding author. Tel.: +43 512 507 5240; fax: +43 512 507 2892.
E-mail address: kathrin.breuker@uibk.ac.at (K. Breuker).

1387-3806
doi:10.1016/j.ijms.2010.05.024

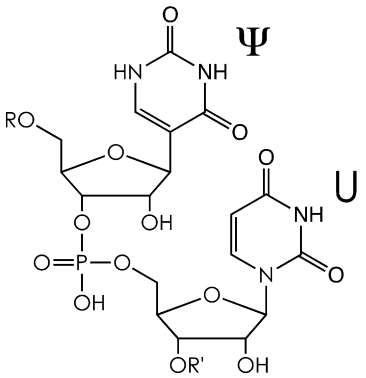

Scheme 1. RNA primary structure with Ψ and U residues; note the C-glycosidic bond of Ψ and the N-glycosidic bond of U.

We report here a new method for detection, localization, and relative quantitation of Ψ in RNA consisting of ∼20 nt by direct monitoring of pseudouridylation sites in CAD experiments. Complete sequence information (without distinguishing between U and Ψ) of the RNA under study is obtained by top–down mass spectrometry. Next, a reference sequence with U in all potential Ψ positions can be synthesized. The two RNAs are hydrolyzed under basic conditions, and products that include the original 3′-terminus and U or Ψ at the 5′-terminus are subjected to low-energy CAD. From nucleobase and nucleoside loss patterns, our approach identifies and localizes Ψ. Of particular importance, we demonstrate that the extent of pseudouridylation can be quantified from CAD spectra of mixtures of sample and reference sequences.

2. Experimental

RNA was prepared using a solid phase synthesis approach [15,16], followed by HPLC purification and desalting using vivaspin 500 centrifugal concentrators (Sartorius, Göttingen, Germany; PES membrane, MWCO 3000). Pseudouridine building blocks for solid phase synthesis were synthesized as described in Refs. [17] and [18]. The 22 nt RNA sequences studied here were GGACG AUACG CGUGA AGCGU CC ("U-sequence") and GGACG AΨACG CGUGA AGCGU CC ("Ψ-sequence"), with hydroxyl groups at the 3′- and 5′-termini. Methanol (Acros, Vienna, Austria) was HPLC grade. Triethylamine (puriss p.a., ≥99.5%), piperidine (puriss p.a., ≥99.0%), 1,8-diazabicyclo[5.4.0]undec-7-ene (DBU, puriss ≥99.0%), and 1-cyclohexylpiperazine (CHP, ≥97.0%) were purchased from Sigma–Aldrich (Vienna, Austria). For RNA hydrolysis, 4 μM RNA was incubated in H_2O with 0.4% vol. DBU or 80 mM CHP (pH 10.5 both) at 60 °C for at least 40 min. For ESI, the hydrolysis solution was diluted to 1 μM RNA in 1:1 H_2O/CH_3OH, with 0.1% vol. DBU or 20 mM CHP (pH 9.5 both). For other experiments, ESI solutions were 1 μM RNA in 1:1 H_2O/CH_3OH with 1% vol. triethylamine or an equal mixture of piperidine and imidazole (25 mM each). ESI flow rate was 1.5 μl/min.

MS and MS/MS experiments were performed on a 7 T Fourier transform-ion cyclotron resonance (FT-ICR) mass spectrometer equipped with an electrospray ionization (ESI) source, a hexapole ion cell floated with argon gas for collisionally activated dissociation, and a hollow dispenser cathode for electron detachment dissociation (EDD) experiments. For EDD, precursor ions were isolated in the ICR cell by application of a radiofrequency waveform, and irradiated with electrons (24 eV) emitted from the indirectly heated hollow dispenser cathode (heating current 1.6 A) for 0.3 s. Precursor ion selection in CAD experiments was realized in an *m*/*z*-selective quadrupole located between ion source and collision cell. Collision energies for CAD were adjusted to give 60–80% fragmentation of the precursor ions.

3. Results and discussion

3.1. MS^3 using CAD

As part of our effort to develop a direct, MS based approach without chemical labeling, we investigated the use of three-stage mass spectrometry (MS^3) for detection and localization of Ψ residues in ∼20 nt RNA. Several researchers have noticed that the nucleobase at the 5′-terminus is particularly labile in low energy CAD of (multiply) deprotonated RNA [19–24]. Moreover, base loss is generally favored over backbone dissociation when precursor ion charge is high (>0.5 charges/nt) [21,22]. We reasoned that subjecting highly charged *y*-type ions from CAD (whose structure is the same as that of truncated RNA with OH groups at the 3′- and 5′-termini [14,20]) to a second stage of low energy collisionally activated dissociation should give MS^3 spectra with preferential loss of the base at the 5′-terminus. Only for *y*-type ions carrying Ψ at the 5′-terminus, base loss should not occur due to resistance of the C-glycosidic bond to dissociation.

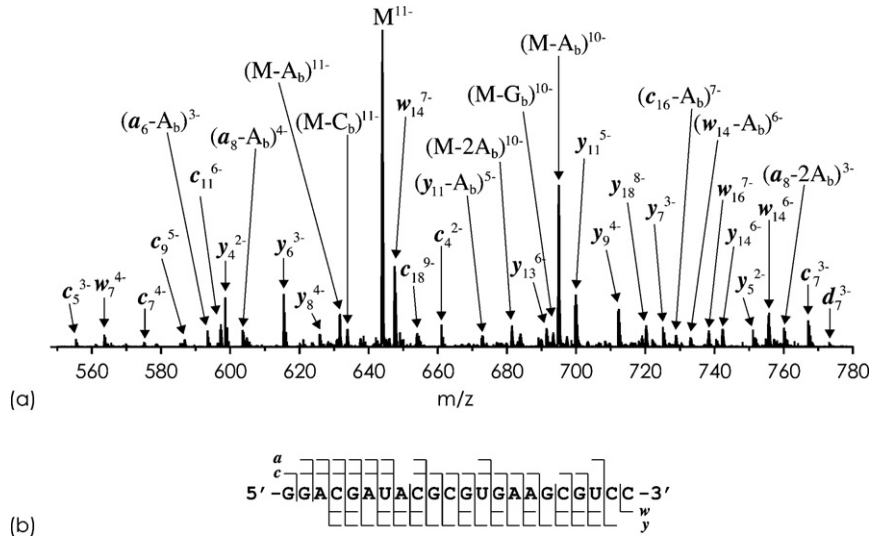

Fig. 1. (a) CAD-MS spectrum of $(M-11H)^{11-}$ ions of 22 nt RNA (U-sequence, 1 μM in 1:1 H_2O/CH_3OH, 1% vol. TEA), laboratory frame collision energy 88 eV; (b) fragment ion map illustrating sequence coverage. A_b, C_b, and G_b stand for nucleobases of adenosine, cytidine, and guanosine, respectively.

However, only 21% of all products from CAD of $(M-11H)^{11-}$ ions (0.5 charges/nt) of 22 nt RNA (Fig. 1) are *y* ions (*a*: 3%, (*a*-base): 17%, *c*: 12%, (*c*-base): 7%, *w*: 10%, (*w*-base): 2%, *y*: 21%, (*y*-base): 2%, internal fragments and base loss from molecular ions: 26%). Signals from y_{20} and y_{21} are completely absent in the CAD spectrum in Fig. 1. Multiple competing dissociation channels as well as secondary fragmentation in CAD of highly charged precursor ions result in *y* ion yields that are insufficient for multiple stages of MS. We conclude that highly charged $(M-nH)^{n-}$ ions are unsuitable as precursors for MS^3 identification and localization of pseudouridine.

In contrast, extensive sequence coverage from *y* ions of relatively high abundance can be obtained in CAD of RNA ions of relatively low charge (~0.2 charges/nt) (Fig. S1). Subjecting lowly charged *y* ions from nozzle skimmer dissociation to CAD gives spectra featuring products from backbone cleavage but little base loss; none of the *y* fragment ions with U at the 5′-terminus of the U-sequence (y_3, y_{10}, y_{16}) dissociates into (*y*-uracil) ions upon collisional activation. Moreover, ratios of *c*, *y*, and *w* ion yields from CAD of the U- and Ψ-sequences show no significant variation with RNA cleavage site at both lower and higher collision energy (Fig. S2);

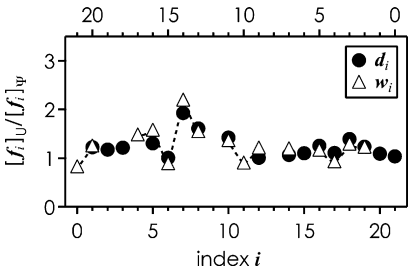

Fig. 2. Ratio of backbone fragment ions f_i from EDD of $(M-11H)^{11-}$ ions of U- and Ψ-sequences (1 μM in 1:1 H_2O/CH_3OH, 1% vol. TEA) versus fragment ion index. The d_i and w_i data are plotted versus the bottom and top axes, respectively. Note that in this plot d_1 corresponds to w_{20}, d_2 to w_{19} etc. to account for the proposed mechanism of EDD backbone fragmentation [25].

replacing U with Ψ in position 7 has no appreciable effect on backbone dissociation. Our data corroborate an important finding by the Schürch group, that RNA dissociation via the *c*/*y* channel is independent of the nucleobase and its glycosidic bond (N–C ver-

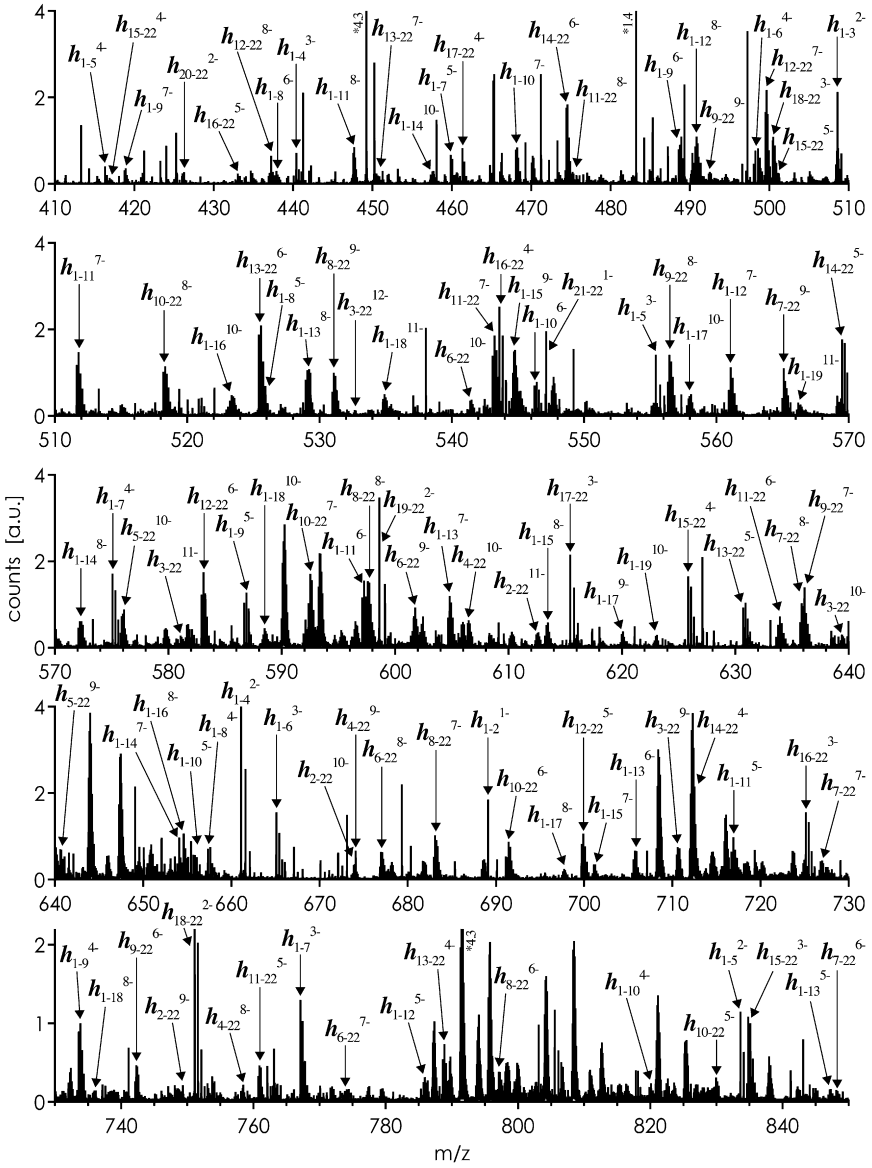

Fig. 3. ESI-MS spectrum of hydrolysis products of 22 nt RNA (U-sequence). For hydrolysis, RNA (4 μM) in aqueous solution at pH 10.5 (0.4% vol. DBU) was incubated at 60 °C for 40 min. For ESI, the hydrolyzed sample was diluted 4-fold, to a concentration corresponding to 1 μM non-hydrolyzed RNA (1:1 H_2O/CH_3OH, 0.1% vol. DBU, pH 9.5).

sus C–C) adjacent to the cleavage site [14,20]. This also rules out RNA ions of relatively low negative net charge as precursors for MS^3 identification and localization of pseudouridine. Nevertheless, data such as those shown in Fig. S1 can be used for de novo sequencing [22,25] (without distinguishing between U and Ψ); with this sequence information, a reference sequence with U in all potential Ψ positions ("U-sequence") can be synthesized.

3.2. MS/MS using EDD

Electron detachment dissociation is a relatively new method for characterization of RNA [25,26]. We have shown recently that backbone fragment ion yields in EDD are correlated with nucleobase ionization energy, and suggested a mechanism for backbone cleavage of RNA [25]. Although ionization energies for Ψ and U residues are not known, we anticipated that possible differences in their ionization energy affect the EDD fragmentation pattern. Fig. 2 shows the ratio of d_i and w_i ions from EDD of the U- and Ψ-sequences versus fragment ion index i. The pseudouridine at position 7 in the Ψ-sequence gives rise to somewhat decreased d_7 and w_{14} fragment ion abundance, corresponding to a relative increase in d_7 and w_{14} from EDD of the U-sequence. This suggests that Ψ has a slightly higher ionization energy than U, and/or that the C-glycosidic bond of Ψ stabilizes the undissociated $(M-11H)^{10-\bullet}$ ions from electron detachment to greater extent than the N-glycosidic bond of U [25]. Anyway, considering the data scatter in Fig. 2, the differences in d and w ion yields are too small to reliably distinguish Ψ from U in EDD experiments.

3.3. Hydrolysis and MS/MS

Bahr et al. reported that acid-catalyzed hydrolysis of ~20 nt RNA can yield almost complete 'mass ladders' consisting of hydrolysis products that include either the original 5′- or 3′-terminus, without interfering products from base losses or multiple backbone hydrolysis [10]. We reasoned that CAD of hydrolysis products including the original 3′-terminus should preferentially give loss of the base at the 5′-terminus when precursor charge is high. ESI of RNA from acidified solutions in negative ion mode, however, produces RNA anions of relatively low net charge; more highly charged ions can be electrosprayed from RNA solutions containing 1% vol. triethylamine (TEA) [25]. We have identified here two more ESI additives for generation of highly charged $(M-nH)^{n-}$ ions of RNA that are also efficient in suppressing salt adducts, and actually give higher ion yields than TEA: 1,8-diazabicyclo[5.4.0]undec-7-ene (DBU) and 1-cyclohexylpiperazine (CHP) (Fig. S3). All three additives (TEA, DBU, CHP) are organic bases, and can be used for base-catalyzed hydrolysis of RNA. We reported recently that base-catalyzed hydrolysis of RNA is generally slower than acid-catalyzed hydrolysis [25]; to save time and speed up hydrolysis, we incubated the basic (pH ~ 10.5) RNA solutions at 60 °C for at least 40 min.

Fig. 3 shows an ESI mass spectrum of products from base-catalyzed hydrolysis of 22 nt RNA (U-sequence). The spectrum shows 'mass ladders' of sequence-informative, highly charged product ions including either the 3′-terminus (h_{i-22}) or the 5′-terminus (h_{1-j}) with i, j = 2–21. Similar spectra are obtained for the Ψ-sequence, consistent with base-catalyzed hydrolysis of the

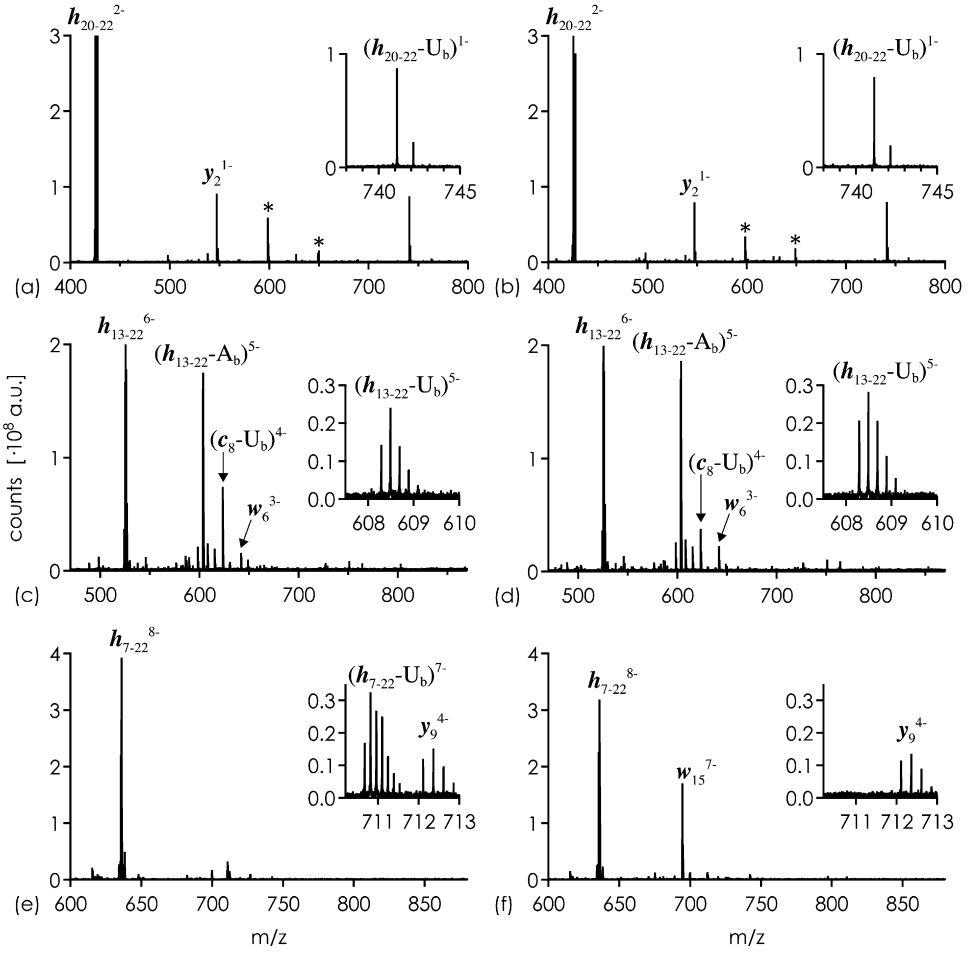

Fig. 4. CAD of hydrolysis products h_{20-22} (UCC), h_{13-22} (UGAAG CGUCC), and h_{7-22} (UACGC GUGAA GCGUC C or ΨACGC GUGAA GCGUC C) from U-sequence (a, c and e) and Ψ-sequence (b, d and f). Laboratory frame collision energy was 18 eV (a and b), 33 eV (c and d), and 48 eV (e and f). Asterisks indicate CAD products from co-isolated hydrolysis products. A_b and U_b stand for nucleobases of adenosine and uridine.

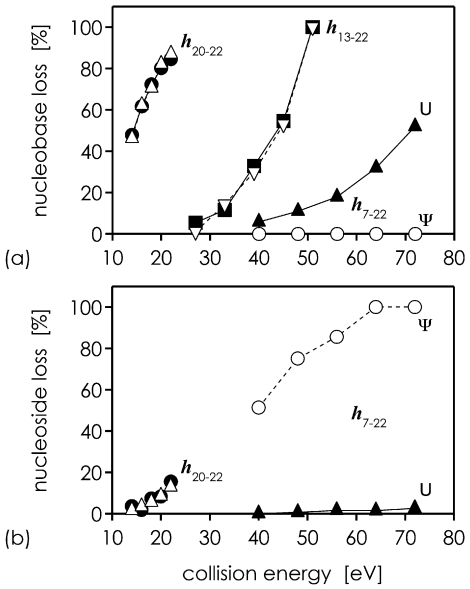

Fig. 5. Percentage of (a) nucleobase (Δm 112.03 Da) and (b) nucleoside loss (Δm 226.06 Da) from U or Ψ at the 5′-terminus in CAD of hydrolysis products $(h_{20-22}-2H)^{2-}$ (△, ●), $(h_{13-22}-6H)^{6-}$ (▽, ■), and $(h_{7-22}-8H)^{8-}$ (○, ▲) versus laboratory frame collision energy. Filled and open symbols represent data for the U- and Ψ-sequence, respectively. All hydrolysis products here have U at the 5′-terminus, except for h_{7-22} from the Ψ-sequence (○), which has Ψ at the 5′-terminus. %-values were calculated relative to h_{i-22} ion abundance (100% = $[h_{i-22}]$ + [(h_{i-22} − nucleobase)] + [(h_{i-22} − nucleoside)]).

phosphodiester backbone being unselective with respect to nucleobase composition [27]. Individual h_{i-22} ions are selected in the linear quadrupole, and subjected to collisionally activated dissociation in the hexapole collision cell. Although in some cases isotopic distributions of the h_{i-22} ions selected for dissociation overlap in m/z with those of other ions, the co-isolated ions generally have different charge values, and CAD products can be assigned unambiguously.

Collisionally activated dissociation of $(h_{20-22}-2H)^{2-}$ (0.67 charges/nt), $(h_{13-22}-6H)^{6-}$ (0.60 charges/nt), and $(h_{7-22}-8H)^{8-}$ (0.5 charges/nt) ions from ESI of hydrolysis products gave the spectra shown in Fig. 4, with data for the U- and Ψ-sequences shown in the left and right columns, respectively. As expected, the CAD spectra of $(h_{20-22}-2H)^{2-}$ and $(h_{13-22}-6H)^{6-}$ from both sequences are virtually identical (Fig. 4a–d). CAD of $(h_{7-22}-8H)^{8-}$ shows clear differences for U or Ψ at the 5′-terminus; charged base loss (Δm = 112.03 Da for U or Ψ) is observed only for the U-sequence (Fig. 4e), but not the Ψ-sequence (Fig. 4f). Contrariwise, $(w_{15}-7H)^{7-}$ ions from CAD of $(h_{7-22}-8H)^{8-}$ are observed only for the Ψ-sequence (Fig. 4f), but not the U-sequence (Fig. 4e). The $(w_{15}-7H)^{7-}$ ions are from loss of the charged nucleoside unit of Ψ; apparently, when the base loss channel is disabled by the C-glycosidic bond, the next favorite channel is loss of the entire nucleoside.

The effect of collision energy on nucleobase and nucleoside loss is shown in Fig. 5. Nucleobase loss is the major dissociation channel in CAD of all hydrolysis products with U at the 5′-terminus. For h_{7-22} with Ψ at the 5′-terminus, the base loss channel is completely inactive at all collision energies studied. Instead, nucleoside loss is the major dissociation channel in CAD of h_{7-22} with Ψ at the 5′-terminus. Nucleoside loss is not observed in CAD of h_{13-22} with U at the 5′-terminus, and is < 20% and <3% for h_{20-22} and h_{7-22} with U at the 5′-terminus, respectively. As expected, no significant difference in dissociation behavior is found for h_{13-22} and h_{20-22} from hydrolysis of the U- and Ψ-sequences. The data for h_{7-22}, however, show that nucleobase loss (Δm 112.03 Da) is diagnostic for U at the 5′-terminus, whereas abundant (>50%) nucleoside loss (Δm 226.06 Da) is diagnostic for Ψ at the 5′-terminus.

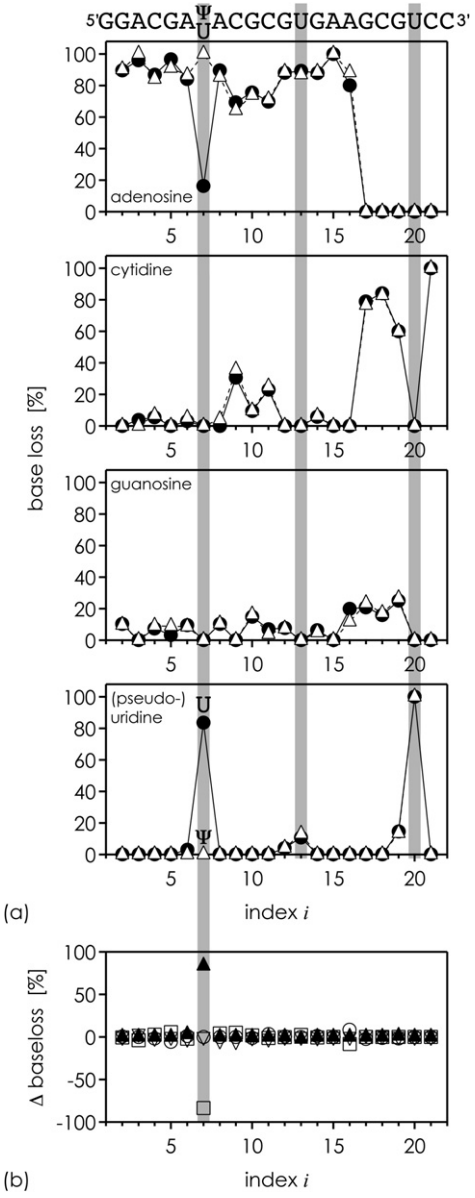

Fig. 6. (a) Percentage of base loss from A (Δm 135.05 Da), C (Δm 111.04 Da), G (Δm 151.05 Da), and U/Ψ (Δm 112.03 Da) in CAD of h_{i-22} from hydrolysis of the U-sequence (circles) and Ψ-sequence (triangles), with 100% = $[h_{i-22} - 135.05] + [h_{i-22} - 111.04] + [h_{i-22} - 151.05] + [h_{i-22} - 112.03]$; the sequence on top is meant to indicate the nucleobase terminating a given hydrolysis product (b) differences between U- and Ψ-sequences in base loss from A (open squares), C (open triangles), G (open circles), and U/Ψ (filled triangles).

Fig. 6a shows percentages of base loss from adenosine, cytidine, guanosine, and uridine or pseudouridine in CAD of products h_{i-22} from hydrolysis of the U- and Ψ-sequences. Loss of adenine is generally favored, but not specific for A at the 5′-terminus of h_{i-22}. In contrast, loss of uracil is observed only from h_{i-22} and $h_{(i-1)-22}$ with U in position i, with ~87% and ~13% uracil loss from h_{i-22} and $h_{(i-1)-22}$, respectively. McLuckey reported that loss of purine bases is favored over loss of pyrimidine bases in CAD of RNA anions [21]. Our data generally agree with this observation, but show increased loss of pyrimidine bases when these are located at the 5′-terminus. Nucleobase loss data for the U- and Ψ-sequences show no significant differences except for i = 7 (Fig. 6b). CAD of h_{7-22} from the U-sequence gives >80% loss of uracil; CAD of h_{7-22} from the Ψ-

sequence gives 0% loss of uracil and 100% loss of adenine instead. Our data show that Ψ can be distinguished from U in CAD experiments of RNA hydrolysis products with Ψ or U at the 5′-terminus by monitoring nucleobase and nucleoside loss.

Naturally, the absence of (h_{i-22}−uracil) ions as positive proof for Ψ at the 5′-terminus requires that collision energy is adjusted such that CAD of the corresponding precursor ions with U at the 5′-terminus would actually give loss of uracil. With unimolecular dissociation depending on ion mass, charge, conformation and base composition, a range of collision energies should be studied to make sure that the absence of (h_{i-22}−uracil) is not caused by insufficient collisional activation. As corroborative evidence, the appearance of abundant (h_{i-22}−uridine) ions shows that activation energy is sufficiently high. However, the most reliable data can be obtained when a reference sequence with U in all potential Ψ positions ('U-sequence') is synthesized, and MS/MS spectra for both the Ψ- and U-sequences are compared.

3.4. Relative quantitation of Ψ

Another important aspect to consider in this context is partial pseudouridylation. RNA from biological samples may show incomplete conversion of uridine into pseudouridine at any given modification site [28], analogous to partial phosphorylation in proteins [29]. In the case of partial pseudouridylation, (h_{i-22}−uracil) as well as (h_{i-22}−uridine) will be observed in CAD spectra of h_{i-22} ions with U or Ψ at the 5′-terminus. As discussed below, these fragment ions can be used for relative quantitation of the extent of site-specific pseudouridylation. The approach proposed here is similar to the method of standard addition in analytical chemistry, and requires synthesis of a reference sequence with U in all potential Ψ sites.

Consider a RNA sequence with n residues, and residue i partially pseudouridylated, with fractions x and $(1-x)$ carrying U and Ψ, respectively ($0 \le x \le 1$). Mixing sample and reference RNA solutions of the same concentration (known from their UV absorption at 260 nm) in various ratios gives mixtures with varying proportions of U and Ψ in position i, without changing the total RNA concentration, i.e., $[\mathrm{RNA}]_{\mathrm{ref}} + [\mathrm{RNA}]_{\mathrm{S}} = C$ is constant. Because base-catalyzed hydrolysis of the phosphodiester backbone does not depend on base composition [27], the h_{i-n} ions from base-catalyzed hydrolysis of the RNA mixtures have the same fractions of U and Ψ at the 5′-terminus. The fraction of RNA with U in position i is $f = [\mathrm{RNA}]_{\mathrm{ref}}/C + x \times [\mathrm{RNA}]_{\mathrm{S}}/C$. With $[\mathrm{RNA}]_{\mathrm{S}} = C - [\mathrm{RNA}]_{\mathrm{ref}}$, we can write $f = [\mathrm{RNA}]_{\mathrm{ref}}/C + x \times (C - [\mathrm{RNA}]_{\mathrm{ref}})/C$, or $f = x + (1-x) \times [\mathrm{RNA}]_{\mathrm{ref}}/C$. As shown above, uracil base loss occurs only from h_{i-n} with U, but not Ψ, at the 5′-terminus. Therefore the abundance of (h_{i-n}−uracil) relative to the added abundances of h_{i-n}, (h_{i-n}−uracil), and (h_{i-n}−uridine), i.e., $[h_{i-n}\text{−uracil}]/([h_{i-n}] + [h_{i-n}\text{−uracil}] + [h_{i-n}\text{−uridine}])$, from low energy CAD of h_{i-n} is directly proportional to f. Finally, normalization of the data with $[h_{i-n}\text{−uracil}]/([h_{i-n}] + [h_{i-n}\text{−uracil}] + [h_{i-n}\text{−uridine}]) = 1$ for CAD of h_{i-n} from the reference sample gives the fraction f of h_{i-n} with U at the 5′-terminus. A plot of f versus the fraction of reference RNA, i.e., $[\mathrm{RNA}]_{\mathrm{ref}}/C$, should then give a straight line with slope $(1-x)$, which intersects the y-axis at x.

To test our approach for relative quantitation of the extent of site-specific pseudouridylation, we prepared three RNA samples with varying U and Ψ content in position 7 of 22 nt RNA by mixing Ψ- and U-sequences in ratios 1:3, 1:1, and 3:1. Fig. 7 shows fractions f determined from CAD of hydrolysis products h_{7-22} for the three samples mixed with varying amounts of reference sample. Within error limits, data obtained at 52 and 56 eV laboratory frame collision energy show no significant differences, and follow closely the proposed function $f = x + (1-x) \times [\mathrm{RNA}]_{\mathrm{ref}}/C$.

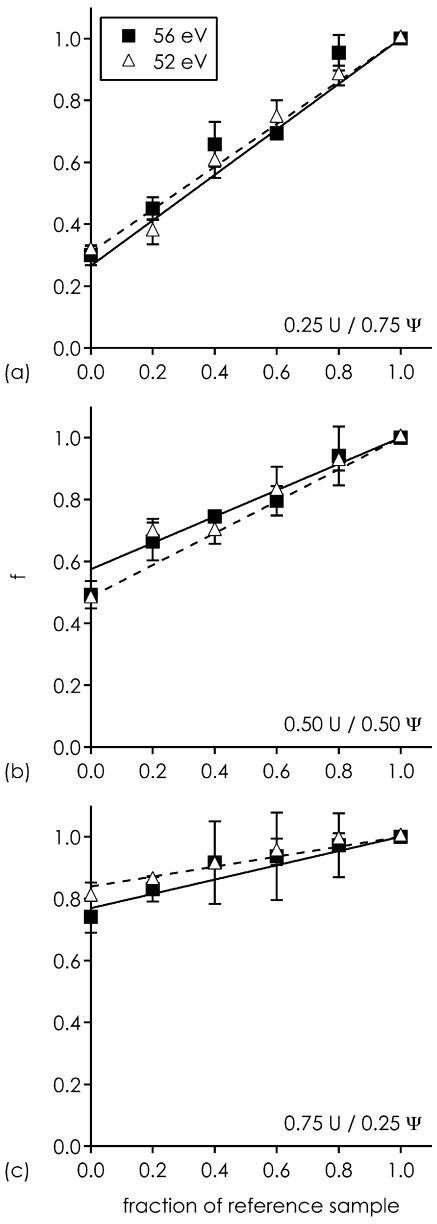

Fig. 7. For h_{7-22} from hydrolysis of 22 nt RNA, fraction f for samples with (a) 25% U/75% Ψ, (b) 50% U/50% Ψ, (c) 75% U/25% Ψ in position 7 calculated from CAD data, versus added fraction of reference RNA (U-sequence). Data points are averages from triplicate measurements, with error bars showing standard deviations. Solid and dashed lines are from weighted fitting of data obtained with 56 and 52 eV laboratory frame collision energy, respectively, using the fit function $f = x + (1-x) \times [\mathrm{RNA}]_{\mathrm{ref}}/C$ derived above.

Table 1
Summary of results from weighted linear least square data fitting shown in Fig. 7; Δ is the difference between measured and actual fractions of U.

Fractions	Collision energy [eV]	Measured fraction of U	Δ
0.25 U/0.75 Ψ	52	0.31	0.06
	56	0.27	0.02
0.50 U/0.50 Ψ	52	0.49	−0.01
	56	0.58	0.08
0.75 U/0.25 Ψ	52	0.84	0.09
	56	0.77	0.02

As summarized in Table 1, the fractions of U at the 5′-terminus of hydrolysis products h_{7-22} from the three test samples determined with our method differ from the actual fractions (0.25, 0.50, 0.75) by less than 0.1. In other words, our method allows determination of pseudouridylation levels to within 10% accuracy. To the best of our knowledge, this is the first report of site-specific relative quantitation of partial pseudouridylation in RNA by mass spectrometry.

4. Conclusions

Our first attempt of using MS^3 for detection and localization of Ψ in RNA turned out to be unsuccessful because highly charged precursor ions give too small *y* ion yields, and lowly charged precursor ions give negligible base loss. We have further investigated the possibility to use electron detachment dissociation for distinguishing between U and Ψ, however, EDD shows only marginal differences in fragmentation pattern for the U- and Ψ-sequences.

In a combined hydrolysis and MS^2 approach, we are able to localize pseudouridylation sites in RNA consisting of 22 nucleotides. We demonstrate that low energy collisionally activated dissociation of highly charged hydrolysis products that include the original 3′-terminus and Ψ or U at the 5′-terminus can be used for unambiguous identification and localization of Ψ. Moreover, by taking advantage of the different fragmentation behavior of Ψ- and U-terminated hydrolysis products, the extent of pseudouridylation can be determined to within 10% accuracy. Our approach is based on mass spectrometry, which offers high sensitivity and the potential for automation. It requires synthesis of a RNA reference sequence, but completely eliminates potential errors from unspecific chemical labeling and complications with reverse-transcriptase reactions. Identification, localization, and relative quantitation of Ψ in larger RNA can potentially be accomplished with our approach after chemical or enzymatic digestion into RNA oligonucleotides consisting of ∼20 nt.

Acknowledgements

We thank Barbara Puffer, Michaela Aigner, Snorri Sigurdsson, and Ronald Micura (R.M.) for discussion, and R.M. for providing the oligonucleotide samples. The Austrian Science Fund is acknowledged for financial support (FWF projects Y372 to K.B. and I317 to R.M.)

Appendix A. Supplementary data

Supplementary data associated with this article can be found, in the online version, at doi:10.1016/j.ijms.2010.05.024.

References

[1] H. Grosjean, R. Benne, Modification and Editing of RNA, American Society for Microbiology, Washington, DC, 1998.
[2] S.C. Pomerantz, J.A. McCloskey, Anal. Chem. 77 (2005) 4687.
[3] T. Hammal, A.R. Ferre-D'Amare, Chem. Biol. 13 (2006) 1125.
[4] A. Durairaj, P.A. Limbach, Anal. Chim. Acta 623 (2008) 117.
[5] A. Bakin, J. Ofengand, Biochemistry 32 (1993) 9754.
[6] K.A. Kellersberger, E. Yu, G.H. Kruppa, M.M. Young, D. Fabris, Anal. Chem. 76 (2004) 2438.
[7] Z.J. Meng, P.A. Limbach, Int. J. Mass Spectrom. 234 (2004) 37.
[8] M. Hossain, P.A. Limbach, RNA 13 (2007) 295.
[9] J. Farand, F. Gosselin, Anal. Chem. 81 (2009) 3723.
[10] U. Bahr, H. Aygun, M. Karas, Anal. Chem. 81 (2009) 3173.
[11] J. Mengel-Jørgensen, F. Kirpekar, Nucleic Acids Res. 30 (2002) e135/1.
[12] F. Kirpekar, L.H. Hansen, A. Rasmussen, J. Poehlsgaard, B. Vester, J. Mol. Biol. 348 (2005) 563.
[13] A. Durairaj, P.A. Limbach, Anal. Chim. Acta 612 (2008) 173.
[14] J.M. Tromp, S. Schürch, Rapid Commun. Mass Spectrom. 20 (2006) 2348.
[15] R. Micura, Angew. Chem. Int. Ed. 41 (2002) 2265.
[16] C. Höbartner, H. Mittendorfer, K. Breuker, R. Micura, Angew. Chem. Int. Ed. 43 (2004) 3922.
[17] B. Puffer, C. Kreutz, U. Rieder, M.O. Ebert, R. Konrat, R. Micura, Nucleic Acids Res. 37 (2009) 7728.
[18] B. Puffer, H. Moroder, M. Aigner, R. Micura, Nucleic Acids Res. 36 (2008) 970.
[19] S. Schürch, E. Bernal-Mendez, C.J. Leumann, J. Am. Soc. Mass Spectrom. 13 (2002) 936.
[20] J.M. Tromp, S. Schürch, J. Am. Soc. Mass Spectrom. 16 (2005) 1262.
[21] T.Y. Huang, A. Kharlamova, J. Liu, S.A. McLuckey, J. Am. Soc. Mass Spectrom. 19 (2008) 1832.
[22] M. Taucher, U. Rieder, K. Breuker, J. Am. Soc. Mass Spectrom. 21 (2010) 278.
[23] J. Wu, S.A. McLuckey, Int. J. Mass Spectrom. 237 (2004) 197.
[24] S. Habibigoudarzi, S.A. Mcluckey, J. Am. Soc. Mass Spectrom. 6 (1995) 102.
[25] M. Taucher, K. Breuker, J. Am. Soc. Mass Spectrom. 21 (2010) 918.
[26] J. Yang, K. Håkansson, J. Am. Soc. Mass Spectrom. 17 (2006) 1369.
[27] P.A. Limbach, Mass Spectrom. Rev. 15 (1996) 297.
[28] X.L. Zhao, Y.T. Yu, RNA 10 (2004) 996.
[29] P.A. Grimsrud, D.L. Swaney, C.D. Wenger, N.A. Beauchene, J.J. Coon, ACS Chem. Biol. 5 (2010) 105.